https://doi.org/10.5194/egusphere-2026-2410
Preprint. Discussion started: 19 May 2026

Satellite Retrieval of Tropospheric NO_2 under Fire Conditions

Mengying Wang[1], Jintai Lin[1], Yuhang Zhang[1], Xiaomeng Jin[2], Wanshan Tan[1], Hao Kong[1], Sijie Wang[1]

[1]Laboratory for Climate and Ocean–Atmosphere Studies, Department of Atmospheric and Oceanic Sciences, School of Physics, Peking University, Beijing 100871, China
[2]Department of Environmental Sciences, Rutgers, The State University of New Jersey, New Brunswick, New Jersey 08901, United States

Correspondence to: Jintai Lin (linjt@pku.edu.cn)

Abstract. Open fires, including wildfires and planned fires, emit large amounts of nitrogen oxides (NO_x = NO + NO_2) into the atmosphere, and their environmental impacts are becoming increasingly severe under climate change. Satellite-based retrievals of tropospheric nitrogen dioxide (NO_2) vertical column densities (VCDs) provide broad spatial coverage and continuous monitoring capabilities for assessing NO_x pollution under fire conditions. However, due to the lack of explicit fire-related a priori information in current satellite NO_2 retrieval algorithms, the resulting data products exhibit large uncertainties under fire conditions. Here, we use the Peking University OMI NO_2 (POMINO) algorithm to investigate the impact of including fire-related a priori information on the tropospheric NO_2 retrieval for the TROPOspheric Monitoring Instrument (TROPOMI) sensor. We conduct sensitivity experiments by including and excluding fire-related a priori information in the NO_2 retrieval process over the western United States in September 2020, a period of intense wildfire activities. The a priori information is taken from GEOS-Chem simulations with and without fire emissions, as well as with different fire emission injection heights. In addition, NO_2 retrieval based on a priori information from the Global Earth Observing System Composition Forecast (GEOS-CF) data is also conducted for comparison. Our results show that including fire-related a priori information in the retrieval significantly increases tropospheric NO_2 VCDs, primarily due to enhanced NO_2 concentrations in the lower layers of the a priori NO_2 profile. Retrieved tropospheric NO_2 VCDs increase by up to 100% at locations greatly impacted by fires and by about 80% in surrounding areas. Differences in fire emission injection height lead to up to ~30% variations in the retrieved VCDs in fire regions, indicating a secondary but non-negligible effect. Validation against EPA surface NO_2 measurements shows improved agreement when fire-related a priori information is included, particularly with lower biases (-12% versus -44%) over fire-affected regions. These results highlight the importance of incorporating fire-related a priori information in satellite NO_2 retrievals to obtain more accurate data for air quality assessments under fire conditions.

1 Introduction

Tropospheric nitrogen oxides (NO_x = NO + NO_2) are important atmospheric pollutants affecting the formation of tropospheric ozone (O_3) and fine particulate matter ($PM_{2.5}$), air quality, and human health (Chameides et al., 1992; Seinfeld and Pandis,

https://doi.org/10.5194/egusphere-2026-2410
Preprint. Discussion started: 19 May 2026

2016; Chen et al., 2022; Southerland et al., 2022). NO_x also influence the atmospheric concentrations of hydroxyl radical (OH) and thus the lifetime of methane (CH_4) (Ehhalt et al., 2001). Approximately 95% of NO_x emissions are released in the form of nitric oxide (NO), and rapid oxidation processes in the atmosphere convert NO to NO_2, reaching a balance within minutes (Jacob, 1999; Solomon, 1999). Therefore, NO_2 is the main form of NO_x in the troposphere, and its VCDs have become a widely-used indicator for diagnosing NO_x pollution and evaluating emission sources (Beirle et al., 2011; Lin and Mcelroy, 2011; Kong et al., 2023; Fioletov et al., 2025a).

Open fires including wildfires and intended burning contribute approximately 15% of global NO_x emissions on an annual basis (Denman et al., 2007). Under climate change, fire frequency and intensity are expected to increase substantially (Senande-Rivera et al., 2022; Burton et al., 2024). For example, even under the low-emission pathway Representative Concentration Pathway 2.6 (RCP2.6), extreme wildfire events are projected to rise by 14%, 30%, and 50% by 2030, 2050, and 2100, respectively (Sullivan et al., 2022). Thus, monitoring NO_2 pollution over fire regions has become increasingly important. Yet fire emissions are highly episodic, spatially heterogeneous, and temporally variable, posing great challenges for their observation and quantification (Van Der Werf et al., 2017; Andreae, 2019). In particular, such strong spatial variability and pronounced temporal randomness are difficult to capture using sparse ground-based observations alone (Chen et al., 2024).

Satellite remote sensing provides an advantageous tool to monitoring tropospheric NO_2 over fire regions, by combining broad spatial coverage with frequent temporal (daily or hourly) sampling that allows large-scale and continuous monitoring. Since the 1990s, many polar-orbiting and geostationary satellite instruments have been launched to monitor NO_2, with continuous advancement in satellite remote sensing technology and refinement of spatial resolution (Burrows et al., 1999; Callies et al., 2000; Levelt et al., 2006; Veefkind et al., 2012; Kim et al., 2020; Nowlan et al., 2025). The TROPOMI provides the highest-spatial-resolution global-scale NO_2 monitoring to date (Van Geffen et al., 2019). Its high spatial resolution allows a refined characterization of NO_2 patterns over fire regions globally, effectively capturing NO_2 signals induced by fire combustion as well as their transport in the atmosphere (Griffin et al., 2021; Jin et al., 2021), provided that proper algorithms to retrieve NO_2 are used under fire conditions.

The retrieval of tropospheric NO_2 VCDs from satellite involves three main steps in general (Boersma et al., 2011). First, the Differential Optical Absorption Spectroscopy (DOAS) technique is applied to fit the measured radiative spectra and derive the total slant column density (SCD) of NO_2 along the effective optical path. Second, a stratosphere–troposphere separation is performed to isolate the tropospheric NO_2 SCD. Finally, the Air Mass Factor (AMF) is calculated using radiative transfer models or look-up tables to convert the tropospheric SCD to the corresponding VCD, with necessary a priori information (on NO_2 vertical profile shape, aerosols, etc.) taken from chemical transport model (CTM) simulations (Palmer et al., 2001; Boersma et al., 2011; Lin et al., 2014; Liu et al., 2020). In heavily polluted regions (such as under fire conditions), retrieval

https://doi.org/10.5194/egusphere-2026-2410
Preprint. Discussion started: 19 May 2026

uncertainties associated with the DOAS fitting and stratosphere-troposphere separation are relatively small, whereas uncertainties related to AMF calculations can reach 30% or more (Lin et al., 2014; Lorente et al., 2017; Boersma et al., 2018).

During the AMF calculation, the dominant sources of uncertainty arise from how the algorithm considers the a priori parameters and assumptions, such as the vertical profile shape of NO_2, the treatment of aerosol optical effects (explicit or implicit), the choice of surface reflectance (Lambertian or angle-dependent), and the determination of clouds (Boersma et al., 2004; Lin et al., 2014; Lorente et al., 2017; Zhang et al., 2025). Under fire conditions, the NO_2 vertical profiles and aerosols exhibit pronounced horizontal and vertical heterogeneity due to the highly localized and episodic nature of fires. This strong spatial variability means that whether fire emissions are accounted for in the a priori NO_2 profile and aerosol information becomes a critical factor for the accuracy of AMF calculations, potentially leading to substantial uncertainties when fires are not properly considered in the retrieval algorithm.

However, the existing NO_2 retrieval algorithms do not adequately consider the effect of open fire emissions on the a priori NO_2 profile and aerosol information. For example, for the OMI and TROPOMI sensors, the QA4ECV v1.1 and TM5-MP-DOMINO algorithms employ the TM5-MP chemical transport model at a spatial resolution of 1° × 1° (Huijnen et al., 2010; Williams et al., 2017; Boersma et al., 2018; Van Geffen et al., 2019). In these two algorithms, fire emissions data are taken from the monthly Global Fire Emissions Database version 3 (GFEDv3) dataset (Van Der Werf et al., 2010), which is subject to time lag. Although the extent of time lag for fires to be accounted for in the TROPOMI operational NO_2 retrieval product (TM5-MP-DOMINO) is not clear, we find that the product exhibits behaviour very similar to our test retrieval using a priori information that exclude fire emissions (see details in Section 3.2). In addition, the relatively coarse spatial resolution of TM5-MP limits its capability in resolving the highly localized and heterogeneous nature of fire events. Furthermore, aerosols are treated in these operational algorithms as “effective clouds” with no explicit corrections. This simplification of aerosol effects may introduce additional uncertainties in regions with high aerosol burdens (Lin et al., 2014; Lin et al., 2015; Liu et al., 2019), such as in the case of fires. Although the official algorithm for TEMPO considers the effect of fire emissions by using a priori information from the GEOS-CF simulations (Keller et al., 2021; Nowlan et al., 2025), its implicit treatment of fire aerosols could affect the accuracy of retrieved NO_2. Thus, improving NO_2 VCD retrievals under fire conditions is essential to properly characterize the impacts of fires on atmospheric composition and air quality.

Here, we use the POMINO retrieval algorithm to investigate the impact of including fire-related a priori information on the retrieval of tropospheric NO_2 VCDs. The POMINO algorithm features an improved treatment of tropospheric NO_2 AMFs (Lin et al., 2014; Lin et al., 2015; Liu et al., 2019; Liu et al., 2020), including the explicit representation of aerosol optical effects, the use of daily bidirectional reflectance distribution function (BRDF) coefficients to account for surface reflectance anisotropy, and relatively high-resolution (25 km) NO_2 profiles. These characteristics make POMINO suitable for conducting sensitivity experiments under fire-induced complex atmospheric conditions. Our sensitivity experiments are conducted for the TROPOMI

https://doi.org/10.5194/egusphere-2026-2410
Preprint. Discussion started: 19 May 2026

sensor in the fire season of September 2020 over the western United States. In consideration of how the existence of fires can affect the NO_2 retrievals, we design experiments of AMF calculation with and without fires as well as experiments setting fire-induced emissions at different heights, which affect the vertical distributions of NO_2 and aerosols. We further use independent ground-based observations to evaluate the retrievals, providing quantitative insight into the importance of improving satellite NO_2 retrievals under open fire conditions.

2 Method and data

2.1 Study domain

The region of study, encompassing California and its surrounding areas (130°W–110°W, 27°N–47°N), is characterized by a dry climate, low cloud fraction, and abundant solar radiation. Forests cover approximately one-third of California's total area, and the pronounced east–west elevation gradient favors the development of hot, dry winds. Together, these factors contribute to the high frequency and intensity of fire events in recent years (Williams et al., 2019; Brodie and Palmer, 2020). Starting from August 2020, persistent drought conditions combined with severe thunderstorms triggered the so-called "2020 Fire Siege", making 2020 one of the most severe wildfire seasons on record (Porter et al., 2020). Notably, the five largest fires of that year (by burned area) all occurred or remained active in September, motivating our focus on this period.

2.2 TROPOMI data and operational retrieval algorithm

The TROPOMI is carried aboard the European Space Agency (ESA) Copernicus Sentinel-5 Precursor (Sentinel-5P) satellite, which was launched on 13 October 2017. Sentinel-5P operates on a near-polar, sun-synchronous orbit with an equator-crossing time of approximately 13:30 local solar time, enabling near-global daily coverage (Veefkind et al., 2012). TROPOMI is dedicated to monitoring the composition of the Earth's atmosphere and measures solar backscattered radiation in eight spectral bands covering the ultraviolet-visible (UVIS), ultraviolet (UV), near-infrared (NIR), and shortwave infrared (SWIR) spectral regions. NO_2 retrievals are performed using measurements in the spectral window from 405 to 465 nm. The instrument provides high spatial-resolution observations, with a nominal nadir pixel size of 3.5 km × 7.0 km prior to 6 August 2019 and 3.5 km × 5.5 km thereafter, much higher than previous instruments. This enhanced spatial resolution substantially improves the capability to detect fine-scale spatial variability in NO_2 concentrations, making TROPOMI particularly suitable for applications over localized emission sources such as open fires.

The official TROPOMI NO_2 product by KNMI is generated with the TM5-MP-DOMINO retrieval algorithm and follows a standard three-step retrieval framework (Eq. 1) mentioned in the introduction. Detailed descriptions of the DOMINO algorithm and the TM5-MP model can be found in previous work (Van Geffen et al., 2019). In the calculation of the tropospheric NO_2 AMF, the algorithm applies an implicit aerosol correction, by assuming aerosols to be "effective clouds" and not explicitly

https://doi.org/10.5194/egusphere-2026-2410
Preprint. Discussion started: 19 May 2026

included in the retrieval process. Surface reflectance is taken from the KNMI TROPOMI DLER v1.0 database at a spatial resolution of 0.5° × 0.5°, which provides a directional surface albedo climatology derived from TROPOMI Level-1b v1.0 measurements (Tilstra et al., 2021). Cloud correction is performed using cloud parameters retrieved by the FRESCO-S algorithm (Wang et al., 2008). The a priori NO_2 vertical profiles are obtained from daily TM5-MP analyses at a horizontal resolution of 1° × 1°. In this study, we use the tropospheric SCD and VCD data from TROPOMI NO_2 RPRO v2.4.0 product.

$$N_V^{trop} = \frac{N_S^{total} - N_S^{strat}}{M} \quad (1)$$

where N_V^{trop} denotes the tropospheric NO_2 VCD, N_S^{total} denotes the total NO_2 SCD retrieved from the DOAS spectral fitting, N_S^{strat} denotes the stratospheric NO_2 SCD obtained from the stratosphere-troposphere separation, and M denotes the tropospheric NO_2 AMF.

Under open fire conditions, the vertical distributions of NO_2, aerosols, and other trace constituents can deviate substantially from those under non-fire conditions (Bousserez, 2014), particularly over remote areas where the NO_2 levels are low under normal conditions. In satellite retrievals of tropospheric NO_2 VCDs, the assumed a priori information therefore constitutes a critical source of uncertainty for both the AMF calculation and the resulting NO_2 VCDs. Within the TM5-MP CTM, fire emissions are taken from the monthly GFEDv3 dataset. Although GFEDv3 data are known to be subject to time lag, the exact implementation of these emissions in the a priori profile construction in TROPOMI NO_2 RPRO v2.4.0 is not clearly documented.

2.3 POMINO retrieval algorithm

In this study, the POMINO retrieval algorithm is employed to assess the impact of fire-related a priori information on satellite retrievals of tropospheric NO_2 VCDs. The POMINO algorithm directly uses the NO_2 SCD data from TROPOMI RPRO v2.4.0 product and focuses on the calculation of tropospheric NO_2 AMFs. The POMINO algorithm performs pixel-by-pixel radiative transfer calculations using the LIDORT v3.6 radiative transfer model with parallel computation, without the use of look-up tables. Thus, it provides a suitable tool to test the effect of fires, explicitly representing how fires affect the vertical profiles of aerosols and NO_2. The POMINO retrieval framework, including how fire conditions are accounted for, is shown in Fig. 1.

https://doi.org/10.5194/egusphere-2026-2410
Preprint. Discussion started: 19 May 2026

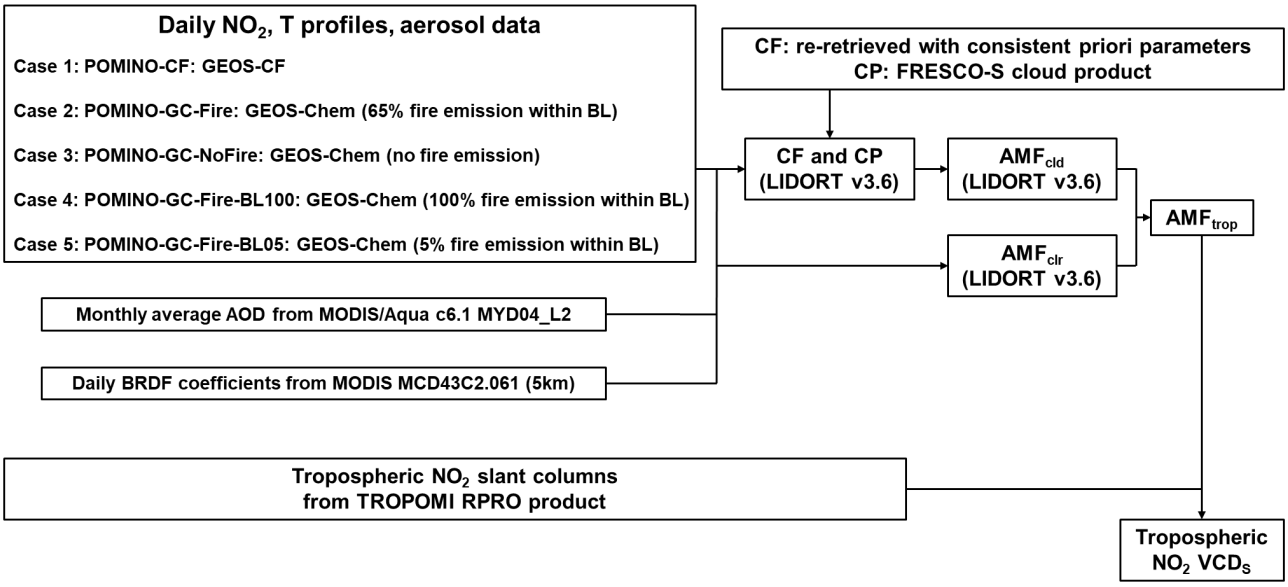

Figure 1. Flowchart of the POMINO retrieval algorithm and its sensitivity experiments. POMINO focuses on the AMF calculation. Colored boxes indicate different a priori information from GEOS-CF, GEOS-Chem simulations with fire emissions (at different heights), and GEOS-Chem simulations without fire emissions. Note that MODIS aerosol optical depth (AOD) is used to constrain the aerosol a priori information, except for the GEOS-Chem simulations without fire emissions. CP denotes cloud-top pressure, and CF denotes effective cloud fraction.

To explicitly characterize aerosols in the AMF calculation, the POMINO algorithm incorporates aerosol information from GEOS-CF (Keller et al., 2021) or our own GEOS-Chem simulations, together with MODIS AOD correction (in the experiments with fires). Meanwhile, daily a priori NO_2 vertical profiles from GEOS-CF or GEOS-Chem simulations are applied. To account for the anisotropy of surface reflectance, the algorithm employs BRDF coefficients from the MODIS MCD43C2.061 product processed at a spatial resolution of 0.05° × 0.05° (Roujean et al., 1992; Zhou et al., 2010). For pixels partially covered by clouds, POMINO applies the independent pixel approximation (IPA) to compute tropospheric NO_2 AMFs (Eq. 2) (Martin et al., 2002). Cloud-top pressure is taken from the official FRESCO-S product, while effective cloud fraction (CF) is recalculated using a priori parameters consistent with the NO_2 retrieval. The cloud layer is assumed to be Lambertian with a fixed reflectance of 0.8.

$$M = w \cdot M_{cld} + (1 - w) \cdot M_{clr} \quad (2)$$

where M denotes the tropospheric NO_2 AMF, w the cloud radiance fraction (CRF), M_{cld} the cloudy-sky AMF, and M_{clr} the clear-sky AMF.

https://doi.org/10.5194/egusphere-2026-2410
Preprint. Discussion started: 19 May 2026

POMINO has been applied to multiple satellite sensors including OMI, TROPOMI, GEMS, and OMS-N (Lin et al., 2014; Lin et al., 2015; Liu et al., 2019; Liu et al., 2020; Zhang et al., 2023; Zhang et al., 2025). For TROPOMI, the algorithm has generated long-term, continuous tropospheric NO_2 VCD datasets over Asia (POMINO-TROPOMI, with the two latest versions being v1.2.2 and v2.1), as well as on a global scale (global POMINO-TROPOMI) (see https://www.pku-atmos-acm.org/acmProduct.php/). Table 1 provides a concise comparison of the key algorithmic treatments and parameters used in the TROPOMI RPRO v2.4.0 product and in the POMINO-TROPOMI v1.2.2 and v2.1 products. POMINO-TROPOMI v2.1 uses a priori NO_2 and aerosol information from the GEOS-CF v1 datasets, replacing the GEOS-Chem v9-02 simulations employed in v1.2.2. Validation against independent MAX-DOAS NO_2 VCD observations demonstrates that POMINO-TROPOMI v2.1 exhibits overall better performance than POMINO-TROPOMI v1.2.2. (Fig. S1). In addition, the global POMINO-TROPOMI NO_2 VCD dataset based on GEOS-CF v1 shows improved agreement with ground-based observations compared with the official TROPOMI NO_2 product (Zhang et al., 2025). Thus, our experiments are conducted based on POMINO-TROPOMI v2.1.

To ensure data quality, the retrieved data are filtered as follows: we exclude pixels with RPRO quality assurance (QA) values $\leqslant 0.5$, solar zenith angle (SZA) or viewing zenith angle (VZA) > 80°, surface albedo > 0.3, or cloud radiance fraction (CRF) > 0.5. The valid Level-2 (pixel-based) NO_2 data are then converted to Level-3 on a 0.05° × 0.05° grid for analysis.

Table 1. Key algorithmic treatments and parameters in the official product and POMINO

Product	RT calculation	Surface reflectance	Aerosol correction	Cloud correction	A priori profiles
TROPOMI RPRO v2.4.0 (official product)	LUT	TROPOMI surface DLER (0.125°, monthly)	Implicit	CP and CF: FRESCO-S	TM5-MP (1°x1°)
POMINO-TROPOMI v1.2.2	LIDORT v3.6	MODIS MCD43C2.061 BRDF (0.05°, 16 days)	Explicit	CP: FRESCO-S CF: re-retrieved	GEOS-Chem v9-02 (0.25°x0.3125°)
POMINO-TROPOMI v2.1	LIDORT v3.6	MODIS MCD43C2.061 BRDF (0.05°,16 days)	Explicit	CP: FRESCO-S CF: re-retrieved	GEOS-CF v1 (0.25°x0.25°)

In the GEOS-CF v1 simulations, fire emissions from the Quick Fire Emissions Dataset version 2.5 (QFED v2.5) dataset are included (Keller et al., 2021). Yet there exist large uncertainties in the amount and height of emissions from each fire event. To quantify the effect of explicit fire treatments on the NO_2 retrieval, we apply the POMINO algorithm to assess the impact

https://doi.org/10.5194/egusphere-2026-2410
Preprint. Discussion started: 19 May 2026

of including or excluding fire-related a priori information and the different settings of fire emission height. We focus on major wildfires that occurred in the western United States in September 2020, with our analysis conducted over the region spanning 130°W–110°W and 27°N–47°N. The sensitivity experiments are summarized in Table 2.

Table 2 Sensitivity experiments for NO_2 retrieval based on the POMINO algorithm

Case	A priori profiles	Fire emission	
POMINO-CF **(same as POMINO-TROPOMI v2.1 and global POMINO-TROPOMI)**	GEOS-CF v1 (0.25°x0.25°)	QFED v2.5	65% within the boundary layer
POMINO-GC-NoFire	GEOS-Chem v12.7.0 (0.25°x0.3125°)	None	
POMINO-GC-Fire	GEOS-Chem v12.7.0 (0.25°x0.3125°)	GFED v4.1	65% within the boundary layer
POMINO-GC-Fire-BL100	GEOS-Chem v12.7.0 (0.25°x0.3125°)	GFED v4.1	100% within the boundary layer
POMINO-GC-Fire-BL05	GEOS-Chem v12.7.0 (0.25°x0.3125°)	GFED v4.1	5% within the boundary layer
POMINO-GC-Fire-CP+50	Same as POMINO-GC-Fire, but with CP increased by 50hPa	Same as POMINO-GC-Fire	Same as POMINO-GC-Fire
POMINO-GC-Fire-CP-50	Same as POMINO-GC-Fire, but with CP decreased by 50hPa	Same as POMINO-GC-Fire	Same as POMINO-GC-Fire

Specifically, the POMINO-CF case uses GEOS-CF v1 data as a priori information, consistent with the POMINO-TROPOMI v2.1 product. Within GEOS-CF v1, fire emissions from the QFED v2.5 dataset are included, with 65% of the emissions allocated within the boundary layer (BL) (Fischer et al., 2014). The GEOS-CF simulation data are obtained from the external data source and do not allow for adjustment of fire emissions required for sensitivity analyses. To explicitly examine the impacts of different fire emission treatments, we conduct a series of GEOS-Chem simulations at a horizontal resolution of 0.25° x 0.3125° with or without GFED v4.1 fire emission data (Jin et al., 2023) and with fire emissions injected at different heights, and use the simulation results of NO_2 profiles and aerosols as a priori information of POMINO. The POMINO-GC-Fire case assumes that 65% of fire emissions are allocated within the BL, similar to the setting in POMINO-CF. The POMINO-

https://doi.org/10.5194/egusphere-2026-2410
Preprint. Discussion started: 19 May 2026

GC-Fire-BL100 and POMINO-GC-Fire-BL05 cases assume 100% and 5% of fire emissions to be located in the BL, respectively, providing two extreme situations of fire injection height. The two cases test how the fire emission height affects the vertical distributions of NO_2 and aerosols and thus the NO_2 retrieval. A lower height, often associated with smaller fires or smoldering, means a larger faction of emissions are released in the BL; and a higher height means fires are more intensive and more emissions are released above the BL. For cloudy pixels, we recalculate the CF with explicit aerosol corrections, but using the CP directly from the FRESCO-S product, which already implicitly includes the effect of aerosols (Van Geffen et al., 2019). To test the effect of this inconsistency and quantify the sensitivity of NO_2 VCD retrievals to uncertainties in CP, we construct two additional cases, POMINO-GC-Fire-CP+50 and POMINO-GC-Fire-CP−50, in which CP is respectively increased and decreased by 50 hPa. Lastly, the POMINO-GC-NoFire case excludes fire-related a priori information by turning off fire emissions in the GEOS-Chem simulations, mimicking the situation in current operational products.

2.4 EPA near-surface NO_2 data

Table 3. Fire region division using VIIRS active fire detections

Region	Definition	Notes
Fire region	Grid cells with detected active fire pixels	Includes isolated and clustered fire pixels
Buffer region	Grid cells surrounding fire regions	Buffer extent depends on the size of contiguous fire clusters: 0 adjacent grid cell for an isolated fire grid cell, 1 adjacent grid cell for clusters of 2–8 grid cells with fire, 3 adjacent grid cells for clusters of ⩾ 9 grid cells with fire
Background region	Grid cells that are neither fire regions nor buffer regions	Represent areas far away from active fire influence

Note: VIIRS active fire detections are aggregated onto a 0.05° × 0.05° grid to match the spatial resolution of the NO_2 VCDs used in the analysis.

https://doi.org/10.5194/egusphere-2026-2410
Preprint. Discussion started: 19 May 2026

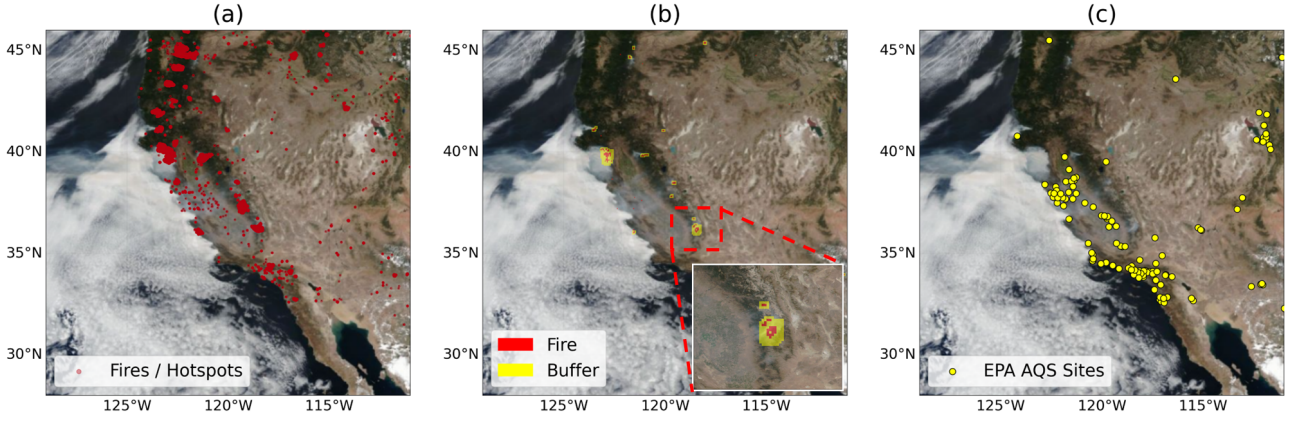

Figure 2. Division of fire regions based on VIIRS active fire detections, and locations of EPA AQS sites. (a) Monthly composite of daytime fire/hotspot detections from the VIIRS Active Fire product. (b) The spatial distribution of fire/hotpot on a single day for example, and the corresponding classification of fire regions (red) and buffer regions (yellow). The inset highlights the buffer definition around fire regions. The detailed classification criteria are provided in Table 3. (c) Locations of EPA AQS sites with valid measurements within ±30 minutes of the TROPOMI overpass time. The true-color satellite basemap is sourced from NASA's Fire Information for Resource Management System (FIRMS) (NASA-FIRMS, 2026).

To evaluate the satellite-retrieved NO_2 VCDs from different experiments, we use near-surface NO_2 mixing ratio measurements from the U.S. Environmental Protection Agency (EPA). Most EPA monitoring stations are located in densely populated urban areas and are generally distant from active fire sources. Nevertheless, these sites may still be influenced by fire emissions through regional transport of fire plumes.

To facilitate the comparison, the NO_2 VCDs are converted to near-surface mixing ratios (Eq. 3) by using the outputs from CTM simulations associated with each experiment:

$$\omega_{surf} = VCD_{trop}^{SAT} \times R^{GC} \times \frac{g \times M}{\Delta p \times N} \times 2 \quad (3)$$

where ω_{surf} denotes the estimated surface NO_2 mixing ratio (in ppb), VCD_{trop}^{SAT} the satellite tropospheric VCD (in molec. cm^{-2}), R^{GC} the GEOS-Chem simulated ratio of NO_2 sub-column in the lowest layer to the total tropospheric column, g the gravity (in m s^{-2}), M the molar mass of NO_2 (in g mol^{-1}), Δp the pressure difference corresponding to the lowest layer (in Pa), and N the Avogadro constant. The thickness of the lowest layer in GEOS-Chem (approximately 130 m) is relatively large, making the layer-averaged NO_2 concentration less representative of the actual near-surface condition measured by the EPA. Therefore, a correction factor of 2 is applied to approximately account for the vertical gradient between the ground level and the midpoint of the model layer (Liu et al., 2018).

https://doi.org/10.5194/egusphere-2026-2410
Preprint. Discussion started: 19 May 2026

To facilitate the evaluation, we identify locations (at the 0.05° × 0.05° grid-cell level) influenced by fire emissions, as follows. In the experiments, the difference in retrieved NO_2 between the POMINO-GC-Fire and POMINO-GC-NoFire cases is caused by whether fire-related a priori information is included. The relative differences between the two cases are predominantly centered around zero, and the number of data points decreases rapidly with increasing relative difference. The relative differences between the two cases follow a generalized normal distribution (Nadarajah, 2005), with an excellent fit ($R^2 = 0.99$, Fig. S2). Based on this fitted distribution, we perform a significance analysis to identify regions with statistically significant differences in retrieved NO_2 due to the inclusion/exclusion of fire emissions at the 95% confidence level. We classify these regions as those influenced by fire emissions. We then compare the satellite-derived near-surface NO_2 mixing ratios with EPA observations separately for regions influenced and not influenced by fire emissions.

2.5 PGN NO_2 VCD data

We further use the Pandonia Global Network (PGN) NO_2 total column product (rnvs3p1-8, https://data.hetzner.pandonia-global-network.org/) to evaluate the satellite-retrieved NO_2. The PGN is a global ground-based observation network designed to provide high-quality measurements of atmospheric reactive trace gases for satellite validation and long-term monitoring (Ialongo et al., 2020; Liu et al., 2024). To ensure spatiotemporal consistency between the ground-based and satellite observations, PGN measurements within 1 h of the TROPOMI overpass time are selected and averaged. This temporal window is chosen to balance the need for sufficient Pandora sampling while minimizing the impact of short-term NO_2 variability. Spatially, the averaged Pandora observations are matched with the mean NO_2 VCDs within a 0.05° radius of each PGN site, which is comparable to the effective spatial footprint of the TROPOMI nadir pixels and reduces representativeness errors caused by spatial heterogeneity (Zhang et al., 2025). To ensure consistency with the tropospheric NO_2 VCDs retrieved from TROPOMI, the stratospheric NO_2 VCDs from the official TROPOMI product are subtracted from the PGN total column measurements, enabling a direct comparison between satellite-retrieved and ground-based tropospheric NO_2 VCDs.

Owing to the limited spatial coverage of PGN sites, within the spatial and temporal domains of this study, only three PGN stations provide valid NO_2 observations suitable for comparison and validation, including Richmond and Mountain View near the San Francisco Bay Area, and Wrightwood near the Los Angeles metropolitan region. The geographic information of these PGN sites is listed in Table S1, and their spatial distribution is shown in Figure S3. All three sites are located near densely populated areas with substantial anthropogenic activity and far away from fire sources, and are therefore are not significantly affected by fires. This characteristic further limits their applicability in our evaluation NO_2 retrievals under fire influences.

https://doi.org/10.5194/egusphere-2026-2410
Preprint. Discussion started: 19 May 2026

3 Results and discussion

3.1 Comparison between POMINO-CF and TM5-MP-DOMINO

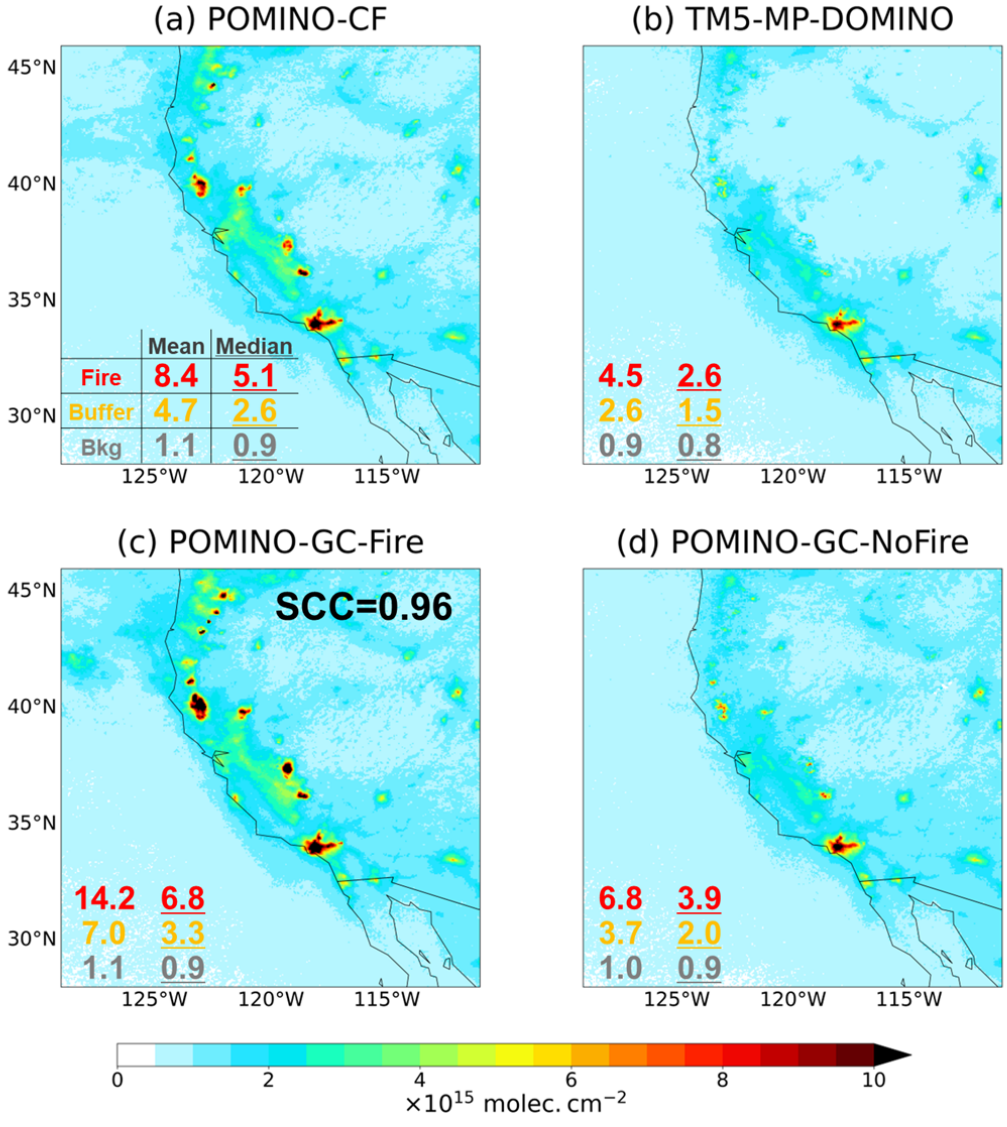

Figure 3. Spatial distribution of monthly mean tropospheric NO_2 VCDs on a 0.05° × 0.05°grid in September 2020. (a) The POMINO-GEOS-CF case, using the GEOS-CF v1 product for a priori information. (b) The official TROPOMI product (RPRO v2.4.0). (c) The POMINO-GC-Fire case. The spatial correlation coefficient (SCC), based on the ranked tropospheric NO_2 VCDs, is computed relative to the POMINO-CF case. (d) The POMINO-GC-NoFire case. Red numbers denote the mean and median NO_2 VCDs within the fire region, yellow numbers denote the mean and median NO_2 VCDs within the buffer region, and grey numbers denote the mean and median NO_2 VCDs within the background region.

https://doi.org/10.5194/egusphere-2026-2410
Preprint. Discussion started: 19 May 2026

The spatial distribution of POMINO-CF monthly mean tropospheric NO_2 VCDs exhibits clear fire-related signals, consistent with the distribution of Visible infrared Imaging Radiometer (VIIRS) fire/hotspots in Fig. 2a. During the study period, widespread and intensive fires in the western United States (Porter et al., 2020) led to markedly elevated NO_2 VCDs over fire-affected regions. Enhanced NO_2 VCDs are also evident in areas downwind of fire clusters, extending over both adjacent land and nearby oceanic regions, consistent with the atmospheric transport of fire-emitted pollutants (Fig. S4). Meanwhile, high NO_2 VCDs are also observed over major urban and industrialized areas in the southwestern United States, such as the Los Angeles metropolitan region, as also shown in the previous work on annual mean NO_2 VCDs based on TROPOMI (Huber et al., 2025) and TEMPO (Fioletov et al., 2025b) instruments. The magnitudes of NO_2 VCDs over these large anthropogenic source regions and fire-affected regions are both substantial, indicating that urban emissions and fires each represent important contributors to tropospheric NO_2 during the study period.

To quantify the spatial extent and intensity of fire impacts, daily VIIRS fire/hotpots data are used to classify the study domain into fire regions, buffer regions, and background regions based on their horizontal distances to fires (see Table 3). We find that the monthly mean POMINO-CF tropospheric NO_2 VCD is 8.4×10^{15} molecules cm^{-2} in fire regions, which is comparable to the annual mean NO_2 VCDs over major urban areas such as Los Angeles (7.5×10^{15} molecules cm^{-2}), 4.7×10^{15} molecules cm^{-2} in buffer regions, and 1.1×10^{15} molecules cm^{-2} in background regions. Pronounced contrasts are evident among the three regions. Relative to background regions, NO_2 VCDs increase by 662% within fire regions and by 331% within buffer regions. These spatial patterns demonstrate that POMINO-CF is able to capture fire-induced NO_2 enhancements, providing a robust basis for quantifying the impacts of fires on regional atmospheric composition.

We further compare the POMINO-CF NO_2 VCDs with the operational TM5-MP-DOMINO product. Here, satellite pixels in each product are screened using their native CRF values, retaining only those with CRF ≤ 0.5. Note that in the TM5-MP-DOMINO algorithm, aerosols are implicitly treated as "effective clouds", therefore the derived CRF represents the combined effects of both clouds and aerosols, and pixels with high aerosol loadings may also be removed as high cloud coverage through the data screening procedure (Lin et al., 2014). This sampling approach leads to a smaller number of valid data points in TM5-MP-DOMINO than in POMINO-CF by 11% in our study domain.

TM5-MP-DOMINO monthly mean NO_2 VCDs are systematically lower than those from POMINO-CF, with the largest discrepancies occurring over fire-affected regions in the western United States. Specifically, NO_2 VCDs retrieved by POMINO-CF are higher than those from TM5-MP-DOMINO in fire regions (by 3.9×10^{15} molecules cm^{-2}) and in buffer regions (by 2.1×10^{15} molecules cm^{-2}). In TM5-MP-DOMINO, concentrated fire regions in the western United States do not exhibit the pronounced NO_2 VCD enhancements (above the surrounding pollution levels) captured by POMINO-CF. Instead, TM5-MP-DOMINO often reports higher NO_2 VCDs over major urban centers than over fire regions. The NO_2 differences

https://doi.org/10.5194/egusphere-2026-2410
Preprint. Discussion started: 19 May 2026

between TM5-MP-DOMINO and POMINO-CF arise from the differences in the treatment of fires (i.e., without versus with) as well as in other assumptions such as aerosol correction (implicit versus explicit), surface reflectance treatment, and radiative transfer calculation (with versus without look-up table). In the following sections, additional experiments are conducted to quantify the effects of fire treatment alone.

3.2 Effects of fire-related a priori information

To more clearly isolate the influence of fire-related a priori information, we conduct sensitivity experiments using the same POMINO retrieval framework combined with GEOS-Chem simulations that either include fire emissions (GEOS-Chem-Fire) or exclude them (GEOS-Chem-NoFire). We then examine the consistency in the a priori information between GEOS-Chem-Fire, GEOS-Chem-NoFire and GEOS-CF, as well as the respective retrieved NO_2 VCDs.

Figure 4 shows the vertical profiles of aerosol extinction and NO_2 over the fire event (RED SALMON COMPLEX). The GEOS-CF data exhibit pronounced enhancements of both aerosol extinction and NO_2 concentrations in the lower troposphere, reflecting the strong influence of fire emissions. In addition, enhanced aerosol extinction and NO_2 concentrations are also present at higher altitudes, likely associated with vertically transported smoke plumes or those transported from upstream fire sources. The GEOS-Chem-Fire simulation reproduces these key features, showing clear fire-related enhancements in both aerosols and NO_2. Compared with GEOS-CF, the GEOS-Chem-Fire exhibits a more surface-confined NO_2 distribution, likely related to different fire emission inputs (GFED v4.1 versus QFED v2.5) as well as differences in boundary-layer mixing and vertical transport schemes (Lin and Mcelroy, 2010; Koster et al., 2015; Van Der Werf et al., 2017; Keller et al., 2021). In contrast, the GEOS-Chem-NoFire simulation shows no pronounced vertical gradients in either aerosols or NO_2, with little pollution across atmospheric layers. This indicates that, without fire emissions, the vertical structures of aerosols and NO_2 lack the characteristic enhancements under fire conditions.

https://doi.org/10.5194/egusphere-2026-2410
Preprint. Discussion started: 19 May 2026

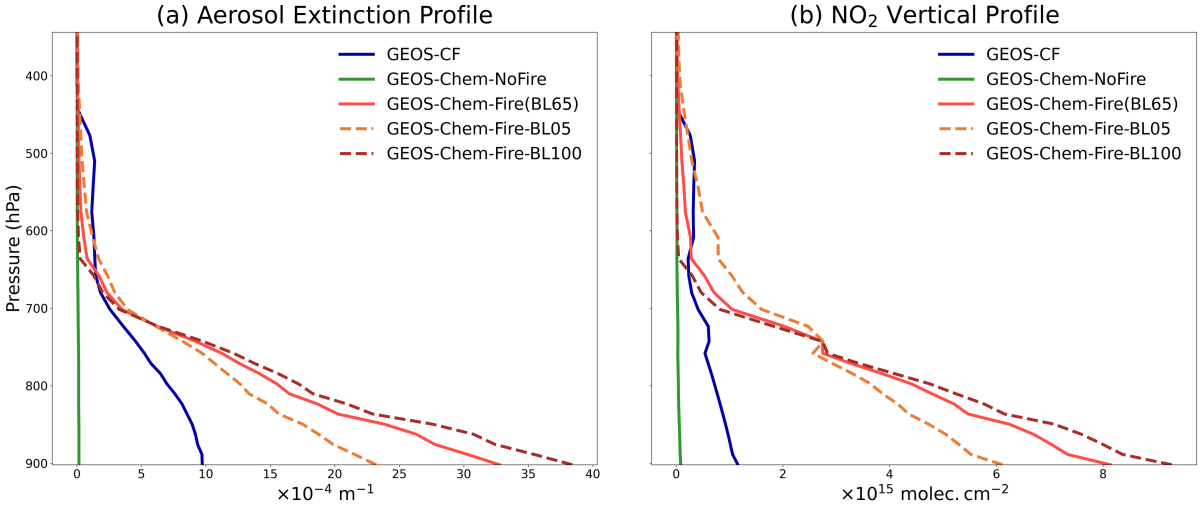

Figure 4. Monthly mean aerosol extinction and NO_2 vertical profiles from different model simulations over the fire event (RED SALMON COMPLEX). (a) Aerosol extinction profiles. (b) NO_2 vertical profiles.

The spatial distribution of retrieved tropospheric NO_2 VCDs in POMINO-GC-Fire closely resembles that of POMINO-CF, with a high spatial correlation coefficient (SCC = 0.96) based on the ranked NO_2 VCDs. Both products capture enhanced NO_2 columns in regions impacted by fires. The regional average NO_2 VCDs in POMINO-GC-Fire are 14.2×10^{15} molecules cm^{-2} in fire regions, 7.0×10^{15} molecules cm^{-2} in buffer regions, and 1.1×10^{15} molecules cm^{-2} in background regions, respectively. These values are generally higher than those derived from POMINO-CF, because NO_2 is more concentrated in the lower troposphere (Fig. 4), leading to smaller AMFs (Boersma et al., 2011).

Note that in both POMINO-CF and POMINO-GC-Fire, there exists a large difference between the mean and median NO_2 VCD in fire regions (Fig. 3), indicating a strongly right-skewed distribution caused by intense fire plumes. The POMINO-GC-Fire case shows the largest mean–median difference, indicating that a small fraction of high-NO_2 grid cells associated with fire emissions substantially elevates the regional mean NO_2 levels. This behavior is consistent with the concentrated and localized NO_2 plumes typically produced by fire emissions. Thus, in terms of median VCD values, POMINO-CF and POMINO-GC-Fire are much closer than the case of mean values (Fig. 3).

By contrast, the spatial distribution of POMINO-GC-NoFire is more consistent with that of TM5-MP-DOMINO, with both products showing pronounced NO_2 enhancements over major urban centers such as the Los Angeles metropolitan area, while maintaining relatively low NO_2 VCDs over fire regions. This similarity suggests that, like POMINO-GC-NoFire, TM5-MP-DOMINO does not effectively include contemporaneous fire-related a priori information. As a result, the vertical distributions

https://doi.org/10.5194/egusphere-2026-2410
Preprint. Discussion started: 19 May 2026

of NO_2 and aerosols associated with fires are not adequately represented, introducing substantial uncertainty into NO_2 VCD retrievals in regions impacted by fires.

These results suggest that both POMINO-CF and POMINO-GC-Fire NO_2 data capture the signal of fire emissions, whereas POMINO-GC-NoFire and TM5-MP-DOMINO do not. Since the only difference in the retrieval process between POMINO-GC-Fire and POMINO-GC-NoFire is the inclusion/exclusion fire-related a priori information, their direct NO_2 comparison effectively quantifies the effects of fire-related a priori information on the retrievals. We found that NO_2 VCDs in POMINO-GC-Fire are much higher than those by POMINO-GC-NoFire in fire regions (by ~100%) and buffer regions (by ~80%). These large differences highlight the importance of explicitly include fire emission a priori information in satellite-based NO_2 retrievals.

3.3 Effects of fire emission injection height

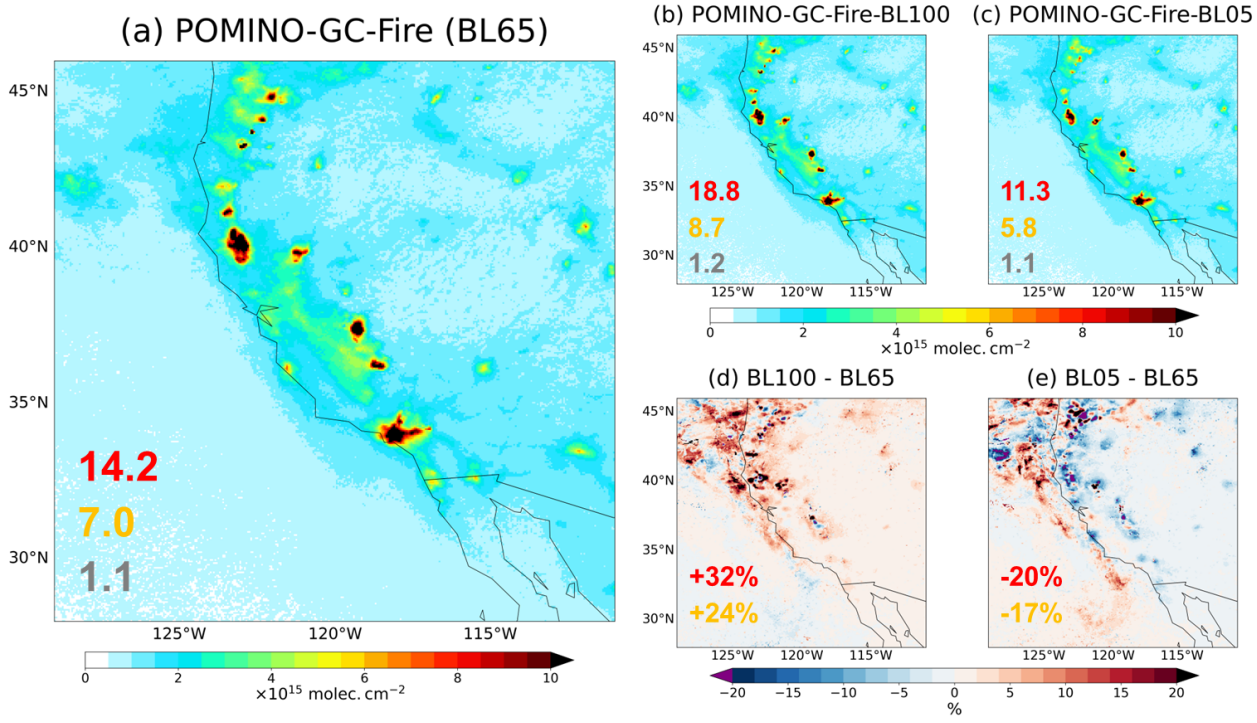

Figure 5. Effects of fire emission injection height on NO_2 retrieval. (a) The spatial distribution of monthly mean NO_2 VCDs in the POMINO-GC-Fire case, with 65% of emissions injected within the boundary layer. (b) The spatial distribution of monthly mean NO_2 VCDs in the POMINO-GC-Fire-BL100 case, with 100% of emissions injected within the boundary layer. (c) The spatial distribution of monthly mean NO_2 VCDs in the POMINO-GC-Fire-BL05 case, with 5% of emissions injected within the boundary layer. (d) Relative differences between POMINO-GC-Fire-BL100 and POMINO-GC-Fire. (e) Relative differences between POMINO-GC-Fire-BL05 and POMINO-GC-Fire. The values in each panel are given for fire regions (red colour), buffer regions (orange colour) and background regions (grey colour).

https://doi.org/10.5194/egusphere-2026-2410
Preprint. Discussion started: 19 May 2026

The assumed emission injection height, affecting the modeled NO_2 vertical profile, affects the retrieved tropospheric NO_2 VCDs, because the AMFs are highly sensitive to the vertical locations of NO_2 and aerosols (Boersma et al., 2011; Lin et al., 2014). To quantify this effect, we compare POMINO-GC-Fire (which assume 65% of fire emissions to be injected in the boundary layer) with POMINO-GC-Fire-BL100 (with 100% of fire emissions injected in the boundary layer) and POMINO-GC-Fire-BL05 (with 5% of fire emissions injected in the boundary layer). Relative to POMINO-GC-Fire, POMINO-GC-Fire-BL100 shows more concentrated NO_2 and aerosols at lower altitudes, leading to smaller AMFs and larger VCDs of NO_2 at the fire source locations. By comparison, GEOS-Chem-Fire-BL05 shifts a larger fraction of the aerosol and NO_2 mass to higher altitudes, resulting in larger AMFs and smaller VCDs of NO_2. For downwind regions, emissions injected at higher altitudes (in POMINO-GC-Fire-BL05) are transported farther to elevate the NO_2 levels there.

When aggregated over the three spatial regions (fire regions, buffer regions, and background regions), the mean NO_2 VCDs consistently follow the order of POMINO-GC-Fire-BL100 > POMINO-GC-Fire (BL65) > POMINO-GC-Fire-BL05. Variations in fire emission injection height can lead to differences in retrieved NO_2 VCDs by approximately 20%–30% in fire regions and buffer regions, indicating a secondary but non-negligible effect. The impacts are relatively small for background regions.

3.4 Impact of cloud-top pressure uncertainties

For cloudy pixels, we directly use the CP data from the FRESCO-S product, but recalculate the CF under explicit aerosol considerations. To test the effect of our imperfect treatment for CP, based on the POMINO-GC-Fire, we construct two additional experiments, POMINO-GC-Fire-CP+50 and POMINO-GC-Fire-CP−50, in which CP is respectively increased and decreased by 50 hPa. As shown in Table 4, across all three regions (fire, buffer and background), perturbing CP by ±50 hPa leads to regional average changes in NO_2 VCD of less than 2%. This small effect is because the cloud fraction is relatively low overall, with a mean CF of 0.02–0.03 from our calculation (or 0.04 in the TROPOMI RPRO v2.4.0), which limits the influence of clouds on the NO_2 retrieval. Under relatively high-CF conditions (with the top 10% of CF values within each region), CP perturbations of ±50 hPa lead to NO_2 VCD changes of approximately 6%–9% across the three regions. Thus, the influence of CP uncertainty on NO_2 retrieval remains significantly smaller than the effect induced by aerosol corrections (implicit versus explicit) (Castellanos et al., 2015; Liu et al., 2019), and is also much smaller than the impact of including or excluding of fire-related a priori information. In addition, the differences among three regions are small, suggesting a spatially consistent response of NO_2 VCD to CP uncertainty. Overall, these results suggest that the imperfect CP treatment does not significantly affect the main conclusions of this study.

https://doi.org/10.5194/egusphere-2026-2410
Preprint. Discussion started: 19 May 2026

Table 4. Sensitivity of NO_2 VCD retrieval to CP. Relative differences are computed against the POMINO-GC-Fire case. Relatively high CF conditions are defined as the top 10% of CF values within each region. CP+50 hPa corresponds to the POMINO-GC-Fire-CP+50 case, and CP-50 hPa corresponds to the POMINO-GC-Fire-CP-50 case.

Region	Overall		Relatively high-CF conditions (top 10%)	
	Mean CF	NO_2 VCD Relative Difference (CP+50hpa, CP-50hpa)	Mean CF	NO_2 VCD Relative Difference (CP+50hpa, CP-50hpa)
Fire	0.03	(-1.2%, 1.3%)	0.13	(-7.5%, 8.8%)
Buffer	0.02	(-1.3%, 1.4%)	0.13	(-7.0%, 7.3%)
Background	0.03	(-1.3%, 1.6%)	0.15	(-5.9%, 6.1%)

4 Validation with ground-based measurements

4.1 Validation with PGN NO_2 VCD measurements

We compare PGN observations with various satellite-derived NO_2 VCD products retrieved with and without fire-related a priori information at three sites (Richmond, Mountain View, and Wrightwood). All satellite products exhibit similar patterns of discrepancy relative to the PGN data (Fig. S5). No systematic separation in magnitude among the different retrieval configurations is evident at these sites. This is likely because these sites are located in areas dominated by anthropogenic emissions and distant from active fires, thus the observed NO_2 columns are primarily controlled by local human activity. Under such conditions, the inclusion or exclusion of contemporaneous fire-related a priori information has little influence on the retrieved NO_2 VCDs.

The systematic discrepancies between satellite and ground-based NO_2 columns likely reflect fundamental differences in measurement sensitivity and spatial representativeness, as well as the inability of coarse satellite footprints and model resolutions to resolve local-scale variability, such as sharp urban emission gradients and small-scale transport processes (Kim et al., 2016; Judd et al., 2019; Li et al., 2023). Given the limited number of PGN sites and their predominantly urban settings within the study domain, this validation exercise does not constitute a comprehensive assessment of retrieval performance under fire conditions.

https://doi.org/10.5194/egusphere-2026-2410
Preprint. Discussion started: 19 May 2026

4.2 Validation with surface NO_2 mixing ratio measurements

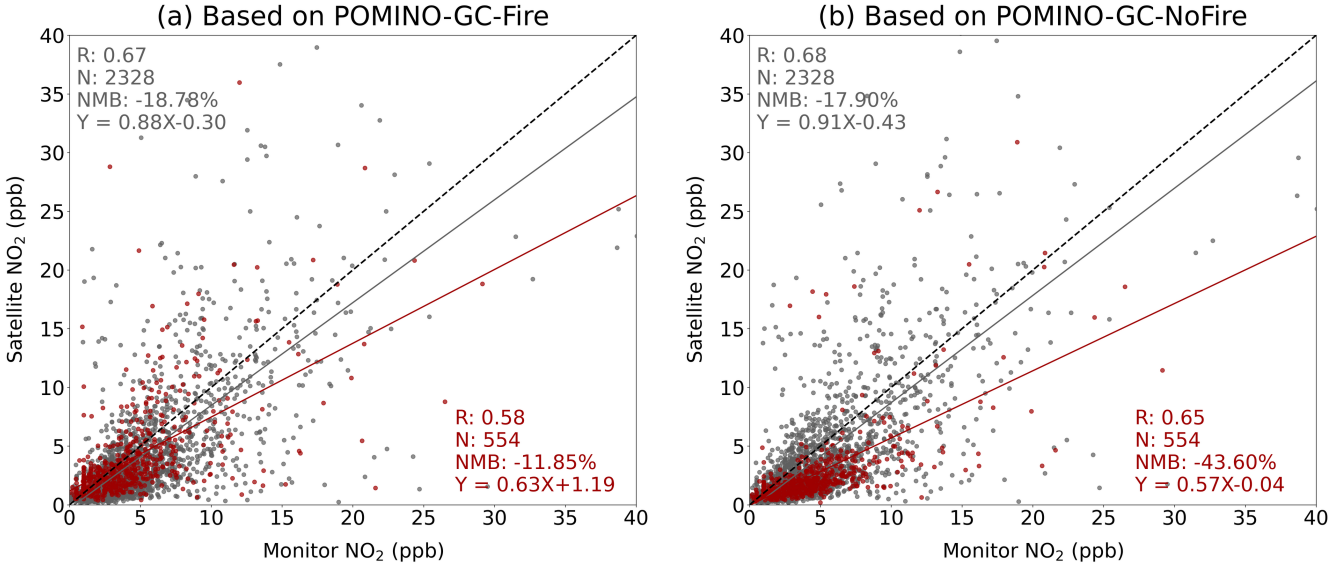

Figure 6. Validation of surface-level NO_2 mixing ratios converted from satellite-derived NO_2 VCDs using EPA in-situ measurements. (a) The scatter plot for NO_2 mixing ratios derived from the POMINO-GC-Fire case versus EPA data. (b) The scatter plot for NO_2 mixing ratios derived from the POMINO-GC-NoFire case versus EPA data. Red points indicate fire-influenced data; and grey points indicate non-fire-influenced data. Statistical metrics are shown in the panels.

Since the PGN observations are insufficient to validate NO_2 VCDs in fire regions, we further employ in situ surface NO_2 mixing ratio measurements from the EPA for additional evaluation. As shown in Section 2.4, satellite-derived tropospheric NO_2 VCDs are converted to near-surface mixing ratios using the GEOS-Chem simulations, and a significance test is applied to identify observations substantially influenced by fire emissions, which are shown in Fig. 6 as red data points.

Figure 6 compares the converted satellite-derived NO_2 mixing ratios with EPA surface observations for retrievals based on (a) POMINO-GC-Fire and (b) POMINO-GC-NoFire. POMINO-GC-Fire exhibits a moderate low bias of −19% at non-fire-affected locations (grey data points) and −12% at fire-affected locations (red data points), indicating that POMINO-GC-Fire maintains good consistency with surface observations under both non-fire and fire conditions. The spatial correlation with EPA data is modest and comparable for both non-fire-affected (0.67) and fire-affected (0.58) cases. In contrast, retrievals based on POMINO-GC-NoFire show notable worsening of bias from −18% at non-fire-affected locations −44% at fire-affected locations, with the retrieved NO_2 data almost always lower than EPA data in fire-affected situations. These results suggest that including fire related a priori information substantially enhances the quality of retrieved NO_2 for regions affected by fires.

https://doi.org/10.5194/egusphere-2026-2410
Preprint. Discussion started: 19 May 2026

5 Conclusions

In this study, we investigate the impact of including fire-related a priori information on the retrieval of tropospheric NO_2 VCDs from satellite observations, given that current operational satellite NO_2 products typically neglect or inadequately represent this information. Using a series of sensitivity experiments based on GEOS-Chem simulations with and without fire emissions and with fire emissions injected at different heights, we quantitatively assess the influence of fire-related a priori information in NO_2 VCDs retrievals in the fire season of September 2020 over the western United States. Our results demonstrate that the inclusion or exclusion of fire-related a priori information can lead to large differences in retrieved NO_2 VCDs, reaching approximately 100% over fire regions. In addition, differences in assumed fire emission injection height lead to smaller, though still non-negligible, variations of up to ~30% at fire regions.

Independent validation using ground-based observations further reveals the importance of including fire-related a priori information for NO_2 retrievals. Although the PGN NO_2 VCDs data available at three sites are insufficient to evaluate the effect of such an inclusion, comparisons with EPA surface NO_2 measurements show that retrievals including fire emissions (POMINO-GC-Fire) better capture the observed NO_2 levels, particularly at fire-affected locations. In contrast, retrievals excluding fire emissions (POMINO-GC-NoFire) exhibit substantial low biases when fire influence is present. In addition, our imperfect consideration of CP (i.e., directly adopting the data from FRESCO-S rather than re-retrieving it) does not result in a substantial impact on the retrieved NO_2 because of low cloud coverage, as is typical for dry and fire-conducive conditions.

Explicitly including fire emissions in the a priori information would become increasingly important to improve the accuracy of satellite-based NO_2 VCD retrievals in the future, as climate change might intensify the fire events. This will require more accurate representations of fire emissions, their injection heights and vertical distributions (Kahn et al., 2008). Such advancements are necessary to better capture the strong spatial and temporal variability of NO_2 associated with fires and to enhance the reliability of satellite observations for air quality monitoring, atmospheric chemistry studies, and assessments of fire-related impacts on human health and climate.

Data availability. The POMINO-TROPOMI NO_2 data is available from the ACM group product website (https://www.pku-atmos-acm.org/acmProduct.php/). The TM5-MP-DOMINO NO_2 product is available from the Copernicus Data Space (https://browser.dataspace.copernicus.eu/). The VIIRS 375 m standard-quality active fire product (fire_archive_SV-C2) from the Suomi-NPP satellite is available via NASA FIRMS (https://firms.modaps.eosdis.nasa.gov/). Surface NO_2 observations from the U.S. Environmental Protection Agency (EPA) air quality monitoring network are available at https://www.epa.gov/outdoor-air-quality-data. The Pandonia Global Network (PGN) NO_2 total column data (rnvs3p1-8) are publicly available at https://data.hetzner.pandonia-global-network.org/

https://doi.org/10.5194/egusphere-2026-2410
Preprint. Discussion started: 19 May 2026

Author contributions. JL conceived this research. MW, JL and YZ designed the algorithm. MW performed all calculations with some code support from YZ and HK. MW and JL wrote the paper. XJ provided GEOS-Chem simulations. WT helped to analyze the simulation data. SW provided support for validation. All authors commented on the paper.

Acknowledgements

The PGN is a bilateral project supported with funding from NASA and ESA. We thank the PI(s), support staff and funding for establishing and maintaining the sites of the PGN used in this investigation.

Financial support

This research is supported by the National Natural Science Foundation of China (grant no. 42430603), and the National Key Research and Development Program of China (grant no. 2023YFC3705802).

References

Andreae, M. O.: Emission of trace gases and aerosols from biomass burning–an updated assessment, Atmospheric Chemistry and Physics, 19, 8523-8546, 2019.

Beirle, S., Boersma, K. F., Platt, U., Lawrence, M. G., and Wagner, T.: Megacity emissions and lifetimes of nitrogen oxides probed from space, Science, 333, 1737-1739, 2011.

Boersma, K., Eskes, H., and Brinksma, E.: Error analysis for tropospheric NO2 retrieval from space, Journal of Geophysical Research: Atmospheres, 109, 2004.

Boersma, K., Eskes, H., Dirksen, R., Van Der A, R., Veefkind, J., Stammes, P., Huijnen, V., Kleipool, Q., Sneep, M., and Claas, J.: An improved tropospheric NO 2 column retrieval algorithm for the Ozone Monitoring Instrument, Atmospheric Measurement Techniques, 4, 1905-1928, 2011.

Boersma, K. F., Eskes, H. J., Richter, A., De Smedt, I., Lorente, A., Beirle, S., Van Geffen, J. H., Zara, M., Peters, E., and Van Roozendael, M.: Improving algorithms and uncertainty estimates for satellite NO 2 retrievals: results from the quality assurance for the essential climate variables (QA4ECV) project, Atmospheric Measurement Techniques, 11, 6651-6678, 2018.

Bousserez, N.: Space-based retrieval of NO 2 over biomass burning regions: quantifying and reducing uncertainties, Atmospheric Measurement Techniques, 7, 3431-3444, 2014.

Brodie, L. C. and Palmer, M.: California's Forest Resources, 2006–2015: Ten-Year Forest Inventory and Analysis Report, Gen. Tech. Rep. PNW-GTR-983. Portland, OR: US Department of Agriculture, Forest Service, Pacific Northwest Research Station. 60 p., 983, 2020.

Burrows, J. P., Weber, M., Buchwitz, M., Rozanov, V., Ladstätter-Weißenmayer, A., Richter, A., DeBeek, R., Hoogen, R., Bramstedt, K., and Eichmann, K.-U.: The global ozone monitoring experiment (GOME): Mission concept and first scientific results, Journal of the Atmospheric Sciences, 56, 151-175, 1999.

https://doi.org/10.5194/egusphere-2026-2410
Preprint. Discussion started: 19 May 2026

Burton, C., Lampe, S., Kelley, D. I., Thiery, W., Hantson, S., Christidis, N., Gudmundsson, L., Forrest, M., Burke, E., and Chang, J.: Global burned area increasingly explained by climate change, Nature Climate Change, 14, 1186-1192, 2024.

Callies, J., Corpaccioli, E., Eisinger, M., Hahne, A., and Lefebvre, A.: GOME-2-Metop's second-generation sensor for operational ozone monitoring, ESA bulletin, 102, 28-36, 2000.

Castellanos, P., Boersma, K., Torres, O., and De Haan, J.: OMI tropospheric NO 2 air mass factors over South America: effects of biomass burning aerosols, Atmospheric Measurement Techniques, 8, 3831-3849, 2015.

Chameides, W., Fehsenfeld, F., Rodgers, M., Cardelino, C., Martinez, J., Parrish, D., Lonneman, W., Lawson, D., Rasmussen, R., and Zimmerman, P.: Ozone precursor relationships in the ambient atmosphere, Journal of Geophysical Research: Atmospheres, 97, 6037-6055, 1992.

Chen, L., Lin, J., Ni, R., Kong, H., Du, M., Yan, Y., Liu, M., Wang, J., Weng, H., and Zhao, Y.: Historical transboundary ozone health impact linked to affluence, Environmental Research Letters, 17, 104014, 2022.

Chen, Y., Morton, D. C., and Randerson, J. T.: Remote sensing for wildfire monitoring: Insights into burned area, emissions, and fire dynamics, One Earth, 7, 1022-1028, 2024.

Denman, K. L., Brasseur, G., Chidthaisong, A., Ciais, P., Cox, P. M., Dickinson, R. E., Hauglustaine, D., Heinze, C., Holland, E., and Jacob, D.: Couplings between changes in the climate system and biogeochemistry, Climate Change 2007: The Physical Science Basis. Contribution of Working Group I to the Fourth Assessment Report of the Intergovernmental Panel on Climate Change The Physical Science Basis, 499-587, 2007.

Ehhalt, D., Prather, M., Dentener, F., Derwent, R., Dlugokencky, E., Holland, E., Isaksen, I., Katima, J., Kirchhoff, V., and Matson, P.: Atmospheric chemistry and greenhouse gases, Climate change 2001: the scientific basis, Intergovernmental panel on climate change, 2001.

Fioletov, V., McLinden, C. A., Griffin, D., Zhao, X., and Eskes, H.: Global seasonal urban, industrial, and background NO2 estimated from TROPOMI satellite observations, Atmospheric Chemistry and Physics, 25, 575-596, 2025a.

Fioletov, V., Griffin, D., McLinden, C. A., Zhao, X., Nowlan, C., and Abad, G. G.: Diurnal variations in background and urban NO2 estimated from TEMPO, Geophysical Research Letters, 52, e2025GL117360, 2025b.

Fischer, E. V., Jacob, D. J., Yantosca, R. M., Sulprizio, M. P., Millet, D., Mao, J., Paulot, F., Singh, H., Roiger, A., and Ries, L.: Atmospheric peroxyacetyl nitrate (PAN): a global budget and source attribution, Atmospheric Chemistry and Physics, 14, 2679-2698, 2014.

Griffin, D., McLinden, C. A., Dammers, E., Adams, C., Stockwell, C., Warneke, C., Bourgeois, I., Peischl, J., Ryerson, T. B., and Zarzana, K. J.: Biomass burning nitrogen dioxide emissions derived from space with TROPOMI: Methodology and validation, Atmospheric Measurement Techniques Discussions, 2021, 1-44, 2021.

Huber, D. E., Kerr, G. H., Nawaz, M. O., Runkel, S., Anenberg, S. C., and Goldberg, D. L.: TROPOMI NO 2 for urban and polluted areas globally from 2019 to 2024, EGUsphere, 2025, 1-33, 2025.

Huijnen, V., Williams, J., van Weele, M., van Noije, T., Krol, M., Dentener, F., Segers, A., Houweling, S., Peters, W., and de Laat, J.: The global chemistry transport model TM5: description and evaluation of the tropospheric chemistry version 3.0, Geoscientific Model Development, 3, 445-473, 2010.

https://doi.org/10.5194/egusphere-2026-2410
Preprint. Discussion started: 19 May 2026

Ialongo, I., Virta, H., Eskes, H., Hovila, J., and Douros, J.: Comparison of TROPOMI/Sentinel-5 Precursor NO 2 observations with ground-based measurements in Helsinki, Atmospheric measurement techniques, 13, 205-218, 2020.

Jacob, D. J.: Introduction to atmospheric chemistry, 1999.

Jin, X., Fiore, A. M., and Cohen, R. C.: Space-based observations of ozone precursors within California wildfire plumes and the impacts on ozone-NO x-VOC chemistry, Environmental Science & Technology, 57, 14648-14660, 2023.

Jin, X., Zhu, Q., and Cohen, R. C.: Direct estimates of biomass burning NO x emissions and lifetimes using daily observations from TROPOMI, Atmospheric Chemistry and Physics, 21, 15569-15587, 2021.

Judd, L. M., Al-Saadi, J. A., Janz, S. J., Kowalewski, M. G., Pierce, R. B., Szykman, J. J., Valin, L. C., Swap, R., Cede, A., and Mueller, M.: Evaluating the impact of spatial resolution on tropospheric NO 2 column comparisons within urban areas using high-resolution airborne data, Atmospheric measurement techniques, 12, 6091-6111, 2019.

Kahn, R. A., Chen, Y., Nelson, D. L., Leung, F. Y., Li, Q., Diner, D. J., and Logan, J. A.: Wildfire smoke injection heights: Two perspectives from space, Geophysical Research Letters, 35, 2008.

Keller, C. A., Knowland, K. E., Duncan, B. N., Liu, J., Anderson, D. C., Das, S., Lucchesi, R. A., Lundgren, E. W., Nicely, J. M., Nielsen, E., Ott, L. E., Saunders, E., Strode, S. A., Wales, P. A., Jacob, D. J., and Pawson, S.: Description of the NASA GEOS Composition Forecast Modeling System GEOS-CF v1.0, Journal of Advances in Modeling Earth Systems, 13, e2020MS002413, https://doi.org/10.1029/2020MS002413, 2021.

Kim, H. C., Lee, P., Judd, L., Pan, L., and Lefer, B.: OMI NO 2 column densities over North American urban cities: the effect of satellite footprint resolution, Geoscientific Model Development, 9, 1111-1123, 2016.

Kim, J., Jeong, U., Ahn, M.-H., Kim, J. H., Park, R. J., Lee, H., Song, C. H., Choi, Y.-S., Lee, K.-H., and Yoo, J.-M.: New era of air quality monitoring from space: Geostationary Environment Monitoring Spectrometer (GEMS), Bulletin of the American Meteorological Society, 101, E1-E22, 2020.

Kong, H., Lin, J., Zhang, Y., Li, C., Xu, C., Shen, L., Liu, X., Yang, K., Su, H., and Xu, W.: High natural nitric oxide emissions from lakes on Tibetan Plateau under rapid warming, Nature Geoscience, 16, 474-477, 2023.

Koster, R. D., Darmenov, A. S., and da Silva, A. M.: The Quick Fire Emissions Dataset (QFED): Documentation of Versions 2.1, 2.2 and 2.4, NASA Goddard Space Flight Center Greenbelt, MD, United States, 2015.

Levelt, P. F., Van Den Oord, G. H., Dobber, M. R., Malkki, A., Visser, H., De Vries, J., Stammes, P., Lundell, J. O., and Saari, H.: The ozone monitoring instrument, IEEE Transactions on geoscience and remote sensing, 44, 1093-1101, 2006.

Li, C., Martin, R. V., Cohen, R. C., Bindle, L., Zhang, D., Chatterjee, D., Weng, H., and Lin, J.: Variable effects of spatial resolution on modeling of nitrogen oxides, Atmospheric Chemistry and Physics, 23, 3031-3049, 2023.

Lin, J.-T. and McElroy, M. B.: Impacts of boundary layer mixing on pollutant vertical profiles in the lower troposphere: Implications to satellite remote sensing, Atmospheric Environment, 44, 1726-1739, 2010.

Lin, J.-T. and McElroy, M. B.: Detection from space of a reduction in anthropogenic emissions of nitrogen oxides during the Chinese economic downturn, Atmospheric Chemistry and Physics, 11, 8171-8188, 2011.

https://doi.org/10.5194/egusphere-2026-2410
Preprint. Discussion started: 19 May 2026

Lin, J.-T., Liu, M.-Y., Xin, J.-Y., Boersma, K., Spurr, R., Martin, R., and Zhang, Q.: Influence of aerosols and surface reflectance on satellite NO 2 retrieval: seasonal and spatial characteristics and implications for NO x emission constraints, Atmospheric Chemistry and Physics, 15, 11217-11241, 2015.

Lin, J.-T., Martin, R., Boersma, K., Sneep, M., Stammes, P., Spurr, R., Wang, P., Van Roozendael, M., Clémer, K., and Irie, H.: Retrieving tropospheric nitrogen dioxide from the Ozone Monitoring Instrument: effects of aerosols, surface reflectance anisotropy, and vertical profile of nitrogen dioxide, Atmospheric Chemistry and Physics, 14, 1441-1461, 2014.

Liu, M., Lin, J., Boersma, K. F., Pinardi, G., Wang, Y., Chimot, J., Wagner, T., Xie, P., Eskes, H., and Van Roozendael, M.: Improved aerosol correction for OMI tropospheric NO 2 retrieval over East Asia: constraint from CALIOP aerosol vertical profile, Atmospheric Measurement Techniques, 12, 1-21, 2019.

Liu, M., Lin, J., Kong, H., Boersma, K. F., Eskes, H., Kanaya, Y., He, Q., Tian, X., Qin, K., and Xie, P.: A new TROPOMI product for tropospheric NO 2 columns over East Asia with explicit aerosol corrections, Atmospheric Measurement Techniques, 13, 4247-4259, 2020.

Liu, M., Lin, J., Wang, Y., Sun, Y., Zheng, B., Shao, J., Chen, L., Zheng, Y., Chen, J., and Fu, T.-M.: Spatiotemporal variability of NO 2 and PM 2.5 over Eastern China: observational and model analyses with a novel statistical method, Atmospheric Chemistry and Physics, 18, 12933-12952, 2018.

Liu, O., Li, Z., Lin, Y., Fan, C., Zhang, Y., Li, K., Zhang, P., Wei, Y., Chen, T., and Dong, J.: Evaluation of the first year of Pandora NO 2 measurements over Beijing and application to satellite validation, Atmospheric Measurement Techniques, 17, 377-395, 2024.

Lorente, A., Folkert Boersma, K., Yu, H., Dörner, S., Hilboll, A., Richter, A., Liu, M., Lamsal, L. N., Barkley, M., and De Smedt, I.: Structural uncertainty in air mass factor calculation for NO 2 and HCHO satellite retrievals, Atmospheric Measurement Techniques, 10, 759-782, 2017.

Martin, R. V., Chance, K., Jacob, D. J., Kurosu, T. P., Spurr, R. J. D., Bucsela, E., Gleason, J. F., Palmer, P. I., Bey, I., Fiore, A. M., Li, Q., Yantosca, R. M., and Koelemeijer, R. B. A.: An improved retrieval of tropospheric nitrogen dioxide from GOME, Journal of Geophysical Research: Atmospheres, 107, 4437, 10.1029/2001jd001027, 2002.

Nadarajah, S.: A generalized normal distribution, Journal of Applied statistics, 32, 685-694, 2005.

NASA-FIRMS: https://firms.modaps.eosdis.nasa.gov/map/, last access: 13 May 2026.

Nowlan, C. R., Abad, G. G., Liu, X., Wang, H., and Chance, K.: TEMPO nitrogen dioxide retrieval algorithm theoretical basis document, NASA Algorithm Publication Tool, 2025.

Palmer, P. I., Jacob, D. J., Chance, K., Martin, R. V., Spurr, R. J., Kurosu, T. P., Bey, I., Yantosca, R., Fiore, A., and Li, Q.: Air mass factor formulation for spectroscopic measurements from satellites: Application to formaldehyde retrievals from the Global Ozone Monitoring Experiment, Journal of Geophysical Research: Atmospheres, 106, 14539-14550, 2001.

2020 Wildfire Activity Statistics: https://www.fire.ca.gov/our-impact/statistics, last access: 12 March 2026.

Roujean, J.-L., Leroy, M., and Deschamps, P.-Y.: A bidirectional reflectance model of the Earth's surface for the correction of remote sensing data, Journal of Geophysical Research: Atmospheres, 97, 20455-20468, https://doi.org/10.1029/92JD01411, 1992.

https://doi.org/10.5194/egusphere-2026-2410
Preprint. Discussion started: 19 May 2026

Seinfeld, J. H. and Pandis, S. N.: Atmospheric chemistry and physics: from air pollution to climate change, John Wiley & Sons2016.

Senande-Rivera, M., Insua-Costa, D., and Miguez-Macho, G.: Spatial and temporal expansion of global wildland fire activity in response to climate change, Nature communications, 13, 1208, 2022.

Solomon, S.: Stratospheric ozone depletion: A review of concepts and history, Reviews of geophysics, 37, 275-316, 1999.

Southerland, V. A., Brauer, M., Mohegh, A., Hammer, M. S., Van Donkelaar, A., Martin, R. V., Apte, J. S., and Anenberg, S. C.: Global urban temporal trends in fine particulate matter (PM2· 5) and attributable health burdens: estimates from global datasets, The Lancet Planetary Health, 6, e139-e146, 2022.

Sullivan, A., Baker, E., Kurvits, T., Popescu, A., Paulson, A. K., Cardinal Christianson, A., Tulloch, A., Bilbao, B., Mathison, C., and Robinson, C.: Spreading like wildfire: The rising threat of extraordinary landscape fires, 2022.

Tilstra, L. G., Tuinder, O. N. E., Wang, P., and Stammes, P.: Directionally dependent Lambertian-equivalent reflectivity (DLER) of the Earth's surface measured by the GOME-2 satellite instruments, Atmos. Meas. Tech., 14, 4219-4238, 10.5194/amt-14-4219-2021, 2021.

Van der Werf, G. R., Randerson, J. T., Giglio, L., Collatz, G., Mu, M., Kasibhatla, P. S., Morton, D. C., DeFries, R., Jin, Y. v., and van Leeuwen, T. T.: Global fire emissions and the contribution of deforestation, savanna, forest, agricultural, and peat fires (1997–2009), Atmospheric chemistry and physics, 10, 11707-11735, 2010.

Van Der Werf, G. R., Randerson, J. T., Giglio, L., Van Leeuwen, T. T., Chen, Y., Rogers, B. M., Mu, M., Van Marle, M. J., Morton, D. C., and Collatz, G. J.: Global fire emissions estimates during 1997–2016, Earth System Science Data, 9, 697-720, 2017.

Van Geffen, J., Eskes, H., Boersma, K., Maasakkers, J., and Veefkind, J.: TROPOMI ATBD of the total and tropospheric NO2 data products (issue 1.4. 0), Royal Netherlands Meteorological Institute (KNMI), De Bilt, the Netherlands, 2019.

Veefkind, J. P., Aben, I., McMullan, K., Förster, H., De Vries, J., Otter, G., Claas, J., Eskes, H., De Haan, J., and Kleipool, Q.: TROPOMI on the ESA Sentinel-5 Precursor: A GMES mission for global observations of the atmospheric composition for climate, air quality and ozone layer applications, Remote sensing of environment, 120, 70-83, 2012.

Wang, P., Stammes, P., Van Der A, R., Pinardi, G., and Van Roozendael, M.: FRESCO+: An improved O 2 A-band cloud retrieval algorithm for tropospheric trace gas retrievals, Atmospheric Chemistry and Physics, 8, 6565-6576, 2008.

Williams, A. P., Abatzoglou, J. T., Gershunov, A., Guzman-Morales, J., Bishop, D. A., Balch, J. K., and Lettenmaier, D. P.: Observed impacts of anthropogenic climate change on wildfire in California, Earth's Future, 7, 892-910, 2019.

Williams, J. E., Boersma, K. F., Le Sager, P., and Verstraeten, W. W.: The high-resolution version of TM5-MP for optimized satellite retrievals: Description and validation, Geoscientific Model Development, 10, 721-750, 2017.

Zhang, Y., Lin, J., Kim, J., Lee, H., Park, J., Hong, H., Van Roozendael, M., Hendrick, F., Wang, T., and Wang, P.: Pomino-gems: A research product for tropospheric NO2 columns from geostationary environment monitoring spectrometer, Atmos. Meas. Tech. Discuss, 2023, 1-28, 2023.

https://doi.org/10.5194/egusphere-2026-2410
Preprint. Discussion started: 19 May 2026

Zhang, Y., Yu, H., De Smedt, I., Lin, J., Theys, N., Van Roozendael, M., Pinardi, G., Compernolle, S., Ni, R., and Ren, F.: Global retrieval of TROPOMI tropospheric HCHO and NO 2 columns with improved consistency based on the updated Peking University OMI NO 2 algorithm, Atmospheric Measurement Techniques, 18, 1561-1589, 2025.

Zhou, Y., Brunner, D., Spurr, R. J. D., Boersma, K. F., Sneep, M., Popp, C., and Buchmann, B.: Accounting for surface reflectance anisotropy in satellite retrievals of tropospheric NO₂, Atmos. Meas. Tech., 3, 1185-1203, 10.5194/amt-3-1185-2010, 2010.